

UC Berkeley

UC Berkeley Previously Published Works

Title

Measurement of ratios of branching fractions and CP-violating asymmetries of $B^\pm \rightarrow D^* K^\pm$ decays

Permalink

<https://escholarship.org/uc/item/4j93q6f2>

Journal

Physical Review D - Particles, Fields, Gravitation and Cosmology, 78(9)

ISSN

1550-7998

Authors

Aubert, B
Bona, M
Karyotakis, Y
[et al.](#)

Publication Date

2008-11-10

DOI

10.1103/PhysRevD.78.092002

License

<https://creativecommons.org/licenses/by/4.0/> 4.0

Peer reviewed

Measurement of ratios of branching fractions and CP -violating asymmetries of $B^\pm \rightarrow D^* K^\pm$ decays

B. Aubert,¹ M. Bona,¹ Y. Karyotakis,¹ J. P. Lees,¹ V. Poireau,¹ E. Prencipe,¹ X. Prudent,¹ V. Tisserand,¹ J. Garra Tico,² E. Grauges,² L. Lopez,^{3a,3b} A. Palano,^{3a,3b} M. Pappagallo,^{3a,3b} G. Eigen,⁴ B. Stugu,⁴ L. Sun,⁴ G. S. Abrams,⁵ M. Battaglia,⁵ D. N. Brown,⁵ R. N. Cahn,⁵ R. G. Jacobsen,⁵ L. T. Kerth,⁵ Yu. G. Kolomensky,⁵ G. Kukartsev,⁵ G. Lynch,⁵ I. L. Osipenkov,⁵ M. T. Ronan,^{5,*} K. Tackmann,⁵ T. Tanabe,⁵ C. M. Hawkes,⁶ N. Soni,⁶ A. T. Watson,⁶ H. Koch,⁷ T. Schroeder,⁷ D. Walker,⁸ D. J. Asgeirsson,⁹ T. Cuhadar-Donszelmann,⁸ B. G. Fulsom,⁹ C. Hearty,⁹ T. S. Mattison,⁹ J. A. McKenna,⁹ M. Barrett,¹⁰ A. Khan,¹⁰ L. Teodorescu,¹⁰ V. E. Blinov,¹¹ A. D. Bukin,¹¹ A. R. Buzykaev,¹¹ V. P. Druzhinin,¹¹ V. B. Golubev,¹¹ A. P. Onuchin,¹¹ S. I. Serednyakov,¹¹ Yu. I. Skovpen,¹¹ E. P. Solodov,¹¹ K. Yu. Todyshev,¹¹ M. Bondioli,¹² S. Curry,¹² I. Eschrich,¹² D. Kirkby,¹² A. J. Lankford,¹² P. Lund,¹² M. Mandelkern,¹² E. C. Martin,¹² D. P. Stoker,¹² S. Abachi,¹³ C. Buchanan,¹³ J. W. Gary,¹⁴ F. Liu,¹⁴ O. Long,¹⁴ B. C. Shen,^{14,*} G. M. Vitug,¹⁴ Z. Yasin,¹⁴ L. Zhang,¹⁴ V. Sharma,¹⁵ C. Campagnari,¹⁶ T. M. Hong,¹⁶ D. Kovalskyi,¹⁶ M. A. Mazur,¹⁶ J. D. Richman,¹⁶ T. W. Beck,¹⁷ A. M. Eisner,¹⁷ C. J. Flacco,¹⁷ C. A. Heusch,¹⁷ J. Kroseberg,¹⁷ W. S. Lockman,¹⁷ T. Schalk,¹⁷ B. A. Schumm,¹⁷ A. Seiden,¹⁷ L. Wang,¹⁷ M. G. Wilson,¹⁷ L. O. Winstrom,¹⁷ C. H. Cheng,¹⁸ D. A. Doll,¹⁸ B. Echenard,¹⁸ F. Fang,¹⁸ D. G. Hitlin,¹⁸ I. Narsky,¹⁸ T. Piatenko,¹⁸ F. C. Porter,¹⁸ R. Andreassen,¹⁹ G. Mancinelli,¹⁹ B. T. Meadows,¹⁹ K. Mishra,¹⁹ M. D. Sokoloff,¹⁹ F. Blanc,²⁰ P. C. Bloom,²⁰ W. T. Ford,²⁰ A. Gaz,²⁰ J. F. Hirschauer,²⁰ A. Kreisel,²⁰ M. Nagel,²⁰ U. Nauenberg,²⁰ J. G. Smith,²⁰ K. A. Ulmer,²⁰ S. R. Wagner,²⁰ R. Ayad,^{21,+} A. Soffer,^{21,‡} W. H. Toki,²¹ R. J. Wilson,²¹ D. D. Altenburg,²² E. Feltresi,²² A. Hauke,²² H. Jasper,²² M. Karbach,²² J. Merkel,²² A. Petzold,²² B. Spaan,²² K. Wacker,²² M. J. Kobel,²³ W. F. Mader,²³ R. Nogowski,²³ K. R. Schubert,²³ R. Schwierz,²³ J. E. Sundermann,²³ A. Volk,²³ D. Bernard,²⁴ G. R. Bonneaud,²⁴ E. Latour,²⁴ Ch. Thiebaut,²⁴ M. Verderi,²⁴ P. J. Clark,²⁵ W. Gradl,²⁵ S. Playfer,²⁵ J. E. Watson,²⁵ M. Andreotti,^{26a,26b} D. Bettoni,^{26a} C. Bozzi,^{26a} R. Calabrese,^{26a,26b} A. Cecchi,^{26a,26b} G. Cibinetto,^{26a,26b} P. Franchini,^{26a,26b} E. Luppi,^{26a,26b} M. Negrini,^{26a,26b} A. Petrella,^{26a,26b} L. Piemontese,^{26a} V. Santoro,^{26a,26b} R. Baldini-Ferrolli,²⁷ A. Calcaterra,²⁷ R. de Sangro,²⁷ G. Finocchiaro,²⁷ S. Pacetti,²⁷ P. Patteri,²⁷ I. M. Peruzzi,^{27,§} M. Piccolo,²⁷ M. Rama,²⁷ A. Zallo,²⁷ A. Buzzo,^{28a} R. Contri,^{28a,28b} M. Lo Vetere,^{28a,28b} M. M. Macri,^{28a} M. R. Monge,^{28a,28b} S. Passaggio,^{28a} C. Patrignani,^{28a,28b} E. Robutti,^{28a} A. Santroni,^{28a,28b} S. Tosi,^{28a,28b} K. S. Chaisanguanthum,²⁹ M. Morii,²⁹ R. S. Dubitzky,³⁰ J. Marks,³⁰ S. Schenk,³⁰ U. Uwer,³⁰ V. Klose,³¹ H. M. Lacker,³¹ G. De Nardo,^{32a,32b} L. Lista,^{32a} D. Monorchio,^{32a,32b} G. Onorato,^{32a,32b} C. Sciacca,^{32a,32b} D. J. Bard,³³ P. D. Dauncey,³³ J. A. Nash,³³ W. Panduro Vazquez,³³ M. Tibbetts,³³ P. K. Behera,³⁴ X. Chai,³⁴ M. J. Charles,³⁴ U. Mallik,³⁴ J. Cochran,³⁵ H. B. Crawley,³⁵ L. Dong,³⁵ W. T. Meyer,³⁵ S. Prell,³⁵ E. I. Rosenberg,³⁵ A. E. Rubin,³⁵ Y. Y. Gao,³⁶ A. V. Gritsan,³⁶ Z. J. Guo,³⁶ C. K. Lae,³⁶ A. G. Denig,³⁷ M. Fritsch,³⁷ G. Schott,³⁷ N. Arnaud,³⁸ J. Béquilleux,³⁸ A. D’Orazio,³⁸ M. Davier,³⁸ J. Firmino da Costa,³⁸ G. Grosdidier,³⁸ A. Höcker,³⁸ V. Lepeltier,³⁸ F. Le Diberder,³⁸ A. M. Lutz,³⁸ S. Pruvot,³⁸ P. Roudeau,³⁸ M. H. Schune,³⁸ J. Serrano,³⁸ V. Sordini,^{38,||} A. Stocchi,³⁸ G. Wormser,³⁸ D. J. Lange,³⁹ D. M. Wright,³⁹ I. Bingham,⁴⁰ J. P. Burke,⁴⁰ C. A. Chavez,⁴⁰ J. R. Fry,⁴⁰ E. Gabathuler,⁴⁰ R. Gamet,⁴⁰ D. E. Hutchcroft,⁴⁰ D. J. Payne,⁴⁰ C. Touramanis,⁴⁰ A. J. Bevan,⁴¹ K. A. George,⁴¹ F. Di Lodovico,⁴¹ R. Sacco,⁴¹ M. Sigamani,⁴¹ G. Cowan,⁴² H. U. Flaecher,⁴² D. A. Hopkins,⁴² S. Paramesvaran,⁴² F. Salvatore,⁴² A. C. Wren,⁴² D. N. Brown,⁴³ C. L. Davis,⁴³ K. E. Alwyn,⁴⁴ N. R. Barlow,⁴⁴ R. J. Barlow,⁴⁴ Y. M. Chia,⁴⁴ C. L. Edgar,⁴⁴ G. D. Lafferty,⁴⁴ T. J. West,⁴⁴ J. I. Yi,⁴⁴ J. Anderson,⁴⁵ C. Chen,⁴⁵ A. Jawahery,⁴⁵ D. A. Roberts,⁴⁵ G. Simi,⁴⁵ J. M. Tuggle,⁴⁵ C. Dallapiccola,⁴⁶ S. S. Hertzbach,⁴⁶ X. Li,⁴⁶ E. Salvati,⁴⁶ S. Saremi,⁴⁶ R. Cowan,⁴⁷ D. Dujmic,⁴⁷ P. H. Fisher,⁴⁷ K. Koeneke,⁴⁷ G. Sciolla,⁴⁷ M. Spitznagel,⁴⁷ F. Taylor,⁴⁷ R. K. Yamamoto,⁴⁷ M. Zhao,⁴⁷ S. E. Mclachlin,^{48,*} P. M. Patel,⁴⁸ S. H. Robertson,⁴⁸ A. Lazzaro,^{49a,49b} V. Lombardo,^{49a} F. Palombo,^{49a,49b} J. M. Bauer,⁵⁰ L. Cremaldi,⁵⁰ V. Eschenburg,⁵⁰ R. Godang,^{50,¶} R. Kroeger,⁵⁰ D. A. Sanders,⁵⁰ D. J. Summers,⁵⁰ H. W. Zhao,⁵⁰ M. Simard,⁵¹ P. Taras,⁵¹ F. B. Viaud,⁵¹ H. Nicholson,⁵² M. A. Baak,⁵³ G. Raven,⁵³ H. L. Snoek,⁵³ C. P. Jessop,⁵⁴ K. J. Knoepfel,⁵⁴ J. M. LoSecco,⁵⁴ W. F. Wang,⁵⁴ G. Benelli,⁵⁵ L. A. Corwin,⁵⁵ K. Honscheid,⁵⁵ H. Kagan,⁵⁵ R. Kass,⁵⁵ J. P. Morris,⁵⁵ A. M. Rahimi,⁵⁵ J. J. Regensburger,⁵⁵ S. J. Sekula,⁵⁵ Q. K. Wong,⁵⁵ N. L. Blount,⁵⁶ J. Brau,⁵⁶ R. Frey,⁵⁶ O. Igonkina,⁵⁶ J. A. Kolb,⁵⁶ M. Lu,⁵⁶ R. Rahmat,⁵⁶ N. B. Sinev,⁵⁶ D. Strom,⁵⁶ J. Strube,⁵⁶ E. Torrence,⁵⁶ G. Castelli,^{57a,57b} N. Gagliardi,^{57a,57b} M. Margoni,^{57a,57b} M. Morandin,^{57a} M. Posocco,^{57a} M. Rotondo,^{57a} F. Simonetto,^{57a,57b} R. Stroili,^{57a,57b} C. Voci,^{57a,57b} P. del Amo Sanchez,⁵⁸ E. Ben-Haim,⁵⁸ H. Briand,⁵⁸ G. Calderini,⁵⁸ J. Chauveau,⁵⁸ P. David,⁵⁸ L. Del Buono,⁵⁸ O. Hamon,⁵⁸ Ph. Leruste,⁵⁸ J. Ocariz,⁵⁸ A. Perez,⁵⁸ J. Prendki,⁵⁸ L. Gladney,⁵⁹ M. Biasini,^{60a,60b} R. Covarelli,^{60a,60b} E. Manoni,^{60a,60b} C. Angelini,^{61a,61b} G. Batignani,^{61a,61b} S. Bettarini,^{61a,61b} M. Carpinelli,^{61a,61b,**} A. Cervelli,^{61a,61b} F. Forti,^{61a,61b} M. A. Giorgi,^{61a,61b} A. Lusiani,^{61a,61c} G. Marchiori,^{61a,61b} M. Morganti,^{61a,61b} N. Neri,^{61a,61b} E. Paoloni,^{61a,61b} G. Rizzo,^{61a,61b} J. J. Walsh,^{61a} J. Biesiada,⁶²

D. Lopes Pegna,⁶² C. Lu,⁶² J. Olsen,⁶² A. J. S. Smith,⁶² A. V. Telnov,⁶² F. Anulli,^{63a} E. Baracchini,^{63a,63b} G. Cavoto,^{63a} D. del Re,^{63a,63b} E. Di Marco,^{63a,63b} R. Faccini,^{63a,63b} F. Ferrarotto,^{63a} F. Ferroni,^{63a,63b} M. Gaspero,^{63a,63b} P. D. Jackson,^{63a} L. Li Gioi,^{63a} M. A. Mazzone,^{63a} S. Morganti,^{63a} G. Piredda,^{63a} F. Polci,^{63a,63b} F. Renga,^{63a,63b} C. Voena,^{63a} M. Ebert,⁶⁴ T. Hartmann,⁶⁴ H. Schröder,⁶⁴ R. Waldi,⁶⁴ T. Adye,⁶⁵ B. Franek,⁶⁵ E. O. Olaiya,⁶⁵ W. Roethel,⁶⁵ F. F. Wilson,⁶⁵ S. Emery,⁶⁶ M. Escalier,⁶⁶ L. Esteve,⁶⁶ A. Gaidot,⁶⁶ S. F. Ganzhur,⁶⁶ G. Hamel de Monchenault,⁶⁶ W. Kozanecki,⁶⁶ G. Vasseur,⁶⁶ Ch. Yèche,⁶⁶ M. Zito,⁶⁶ X. R. Chen,⁶⁷ H. Liu,⁶⁷ W. Park,⁶⁷ M. V. Purohit,⁶⁷ R. M. White,⁶⁷ J. R. Wilson,⁶⁷ M. T. Allen,⁶⁸ D. Aston,⁶⁸ R. Bartoldus,⁶⁸ P. Bechtler,⁶⁸ J. F. Benitez,⁶⁸ R. Cenci,⁶⁸ J. P. Coleman,⁶⁸ M. R. Convery,⁶⁸ J. C. Dingfelder,⁶⁸ J. Dorfan,⁶⁸ G. P. Dubois-Felsmann,⁶⁸ W. Dunwoodie,⁶⁸ R. C. Field,⁶⁸ A. M. Gabareen,⁶⁸ S. J. Gowdy,⁶⁸ M. T. Graham,⁶⁸ P. Grenier,⁶⁸ C. Hast,⁶⁸ W. R. Innes,⁶⁸ J. Kaminski,⁶⁸ M. H. Kelsey,⁶⁸ H. Kim,⁶⁸ P. Kim,⁶⁸ M. L. Kocian,⁶⁸ D. W. G. S. Leith,⁶⁸ S. Li,⁶⁸ B. Lindquist,⁶⁸ S. Luitz,⁶⁸ V. Luth,⁶⁸ H. L. Lynch,⁶⁸ D. B. MacFarlane,⁶⁸ H. Marsiske,⁶⁸ R. Messner,⁶⁸ D. R. Muller,⁶⁸ H. Neal,⁶⁸ S. Nelson,⁶⁸ C. P. O'Grady,⁶⁸ I. Ofte,⁶⁸ A. Perazzo,⁶⁸ M. Perl,⁶⁸ B. N. Ratcliff,⁶⁸ A. Roodman,⁶⁸ A. A. Salnikov,⁶⁸ R. H. Schindler,⁶⁸ J. Schwiening,⁶⁸ A. Snyder,⁶⁸ D. Su,⁶⁸ M. K. Sullivan,⁶⁸ K. Suzuki,⁶⁸ S. K. Swain,⁶⁸ J. M. Thompson,⁶⁸ J. Va'vra,⁶⁸ A. P. Wagner,⁶⁸ M. Weaver,⁶⁸ C. A. West,⁶⁸ W. J. Wisniewski,⁶⁸ M. Wittgen,⁶⁸ D. H. Wright,⁶⁸ H. W. Wulsin,⁶⁸ A. K. Yarritu,⁶⁸ K. Yi,⁶⁸ C. C. Young,⁶⁸ V. Ziegler,⁶⁸ P. R. Burchat,⁶⁹ A. J. Edwards,⁶⁹ S. A. Majewski,⁶⁹ T. S. Miyashita,⁶⁹ B. A. Petersen,⁶⁹ L. Wilden,⁶⁹ S. Ahmed,⁷⁰ M. S. Alam,⁷⁰ R. Bula,⁷⁰ J. A. Ernst,⁷⁰ B. Pan,⁷⁰ M. A. Saeed,⁷⁰ S. B. Zain,⁷⁰ S. M. Spanier,⁷¹ B. J. Wogslund,⁷¹ R. Eckmann,⁷² J. L. Ritchie,⁷² A. M. Ruland,⁷² C. J. Schilling,⁷² R. F. Schwitters,⁷² B. W. Drummond,⁷³ J. M. Izen,⁷³ X. C. Lou,⁷³ F. Bianchi,^{74a,74b} D. Gamba,^{74a,74b} M. Pelliccioni,^{74a,74b} M. Bomben,^{75a,75b} L. Bosisio,^{75a,75b} C. Cartaro,^{75a,75b} G. Della Ricca,^{75a,75b} L. Lanceri,^{75a,75b} L. Vitale,^{75a,75b} V. Azzolini,⁷⁶ N. Lopez-March,⁷⁶ F. Martinez-Vidal,⁷⁶ D. A. Milanes,⁷⁶ A. Oyanguren,⁷⁶ J. Albert,⁷⁷ Sw. Banerjee,⁷⁷ B. Bhuyan,⁷⁷ H. H. F. Choi,⁷⁷ K. Hamano,⁷⁷ R. Kowalewski,⁷⁷ M. J. Lewczuk,⁷⁷ I. M. Nugent,⁷⁷ J. M. Roney,⁷⁷ R. J. Sobie,⁷⁷ T. J. Gershon,⁷⁸ P. F. Harrison,⁷⁸ J. Ilic,⁷⁸ T. E. Latham,⁷⁸ G. B. Mohanty,⁷⁸ H. R. Band,⁷⁹ X. Chen,⁷⁹ S. Dasu,⁷⁹ K. T. Flood,⁷⁹ Y. Pan,⁷⁹ M. Pierini,⁷⁹ R. Prepost,⁷⁹ C. O. Vuosalo,⁷⁹ and S. L. Wu⁷⁹

(BABAR Collaboration)

¹Laboratoire de Physique des Particules, IN2P3/CNRS et Université de Savoie, F-74941 Annecy-Le-Vieux, France

²Universitat de Barcelona, Facultat de Física, Departament ECM, E-08028 Barcelona, Spain

^{3a}INFN Sezione di Bari, I-70126 Bari, Italy

^{3b}Dipartimento di Fisica, Università di Bari, I-70126 Bari, Italy

⁴University of Bergen, Institute of Physics, N-5007 Bergen, Norway

⁵Lawrence Berkeley National Laboratory and University of California, Berkeley, California 94720, USA

⁶University of Birmingham, Birmingham, B15 2TT, United Kingdom

⁷Ruhr Universität Bochum, Institut für Experimentalphysik 1, D-44780 Bochum, Germany

⁸University of Bristol, Bristol BS8 1TL, United Kingdom

⁹University of British Columbia, Vancouver, British Columbia, Canada V6T 1Z1

¹⁰Brunel University, Uxbridge, Middlesex UB8 3PH, United Kingdom

¹¹Budker Institute of Nuclear Physics, Novosibirsk 630090, Russia

¹²University of California at Irvine, Irvine, California 92697, USA

¹³University of California at Los Angeles, Los Angeles, California 90024, USA

¹⁴University of California at Riverside, Riverside, California 92521, USA

¹⁵University of California at San Diego, La Jolla, California 92093, USA

¹⁶University of California at Santa Barbara, Santa Barbara, California 93106, USA

¹⁷University of California at Santa Cruz, Institute for Particle Physics, Santa Cruz, California 95064, USA

¹⁸California Institute of Technology, Pasadena, California 91125, USA

¹⁹University of Cincinnati, Cincinnati, Ohio 45221, USA

²⁰University of Colorado, Boulder, Colorado 80309, USA

²¹Colorado State University, Fort Collins, Colorado 80523, USA

²²Technische Universität Dortmund, Fakultät Physik, D-44221 Dortmund, Germany

²³Technische Universität Dresden, Institut für Kern- und Teilchenphysik, D-01062 Dresden, Germany

²⁴Laboratoire Leprince-Ringuet, CNRS/IN2P3, Ecole Polytechnique, F-91128 Palaiseau, France

²⁵University of Edinburgh, Edinburgh EH9 3JZ, United Kingdom

^{26a}INFN Sezione di Ferrara, I-44100 Ferrara, Italy

^{26b}Dipartimento di Fisica, Università di Ferrara, I-44100 Ferrara, Italy

²⁷INFN Laboratori Nazionali di Frascati, I-00044 Frascati, Italy

^{28a}INFN Sezione di Genova, I-16146 Genova, Italy

^{28b}Dipartimento di Fisica, Università di Genova, I-16146 Genova, Italy

- ²⁹Harvard University, Cambridge, Massachusetts 02138, USA
- ³⁰Universität Heidelberg, Physikalisches Institut, Philosophenweg 12, D-69120 Heidelberg, Germany
- ³¹Humboldt-Universität zu Berlin, Institut für Physik, Newtonstr. 15, D-12489 Berlin, Germany
- ^{32a}INFN Sezione di Napoli, I-80126 Napoli, Italy;
- ^{32b}Dipartimento di Scienze Fisiche, Università di Napoli Federico II, I-80126 Napoli, Italy
- ³³Imperial College London, London, SW7 2AZ, United Kingdom
- ³⁴University of Iowa, Iowa City, Iowa 52242, USA
- ³⁵Iowa State University, Ames, Iowa 50011-3160, USA
- ³⁶Johns Hopkins University, Baltimore, Maryland 21218, USA
- ³⁷Universität Karlsruhe, Institut für Experimentelle Kernphysik, D-76021 Karlsruhe, Germany
- ³⁸Laboratoire de l'Accélérateur Linéaire, IN2P3/CNRS et Université Paris-Sud 11, Centre Scientifique d'Orsay, B.P. 34, F-91898 ORSAY Cedex, France
- ³⁹Lawrence Livermore National Laboratory, Livermore, California 94550, USA
- ⁴⁰University of Liverpool, Liverpool L69 7ZE, United Kingdom
- ⁴¹Queen Mary, University of London, E1 4NS, United Kingdom
- ⁴²University of London, Royal Holloway and Bedford New College, Egham, Surrey TW20 0EX, United Kingdom
- ⁴³University of Louisville, Louisville, Kentucky 40292, USA
- ⁴⁴University of Manchester, Manchester M13 9PL, United Kingdom
- ⁴⁵University of Maryland, College Park, Maryland 20742, USA
- ⁴⁶University of Massachusetts, Amherst, Massachusetts 01003, USA
- ⁴⁷Massachusetts Institute of Technology, Laboratory for Nuclear Science, Cambridge, Massachusetts 02139, USA
- ⁴⁸McGill University, Montréal, Québec, Canada H3A 2T8
- ^{49a}INFN Sezione di Milano, I-20133 Milano, Italy
- ^{49b}Dipartimento di Fisica, Università di Milano, I-20133 Milano, Italy
- ⁵⁰University of Mississippi, University, Mississippi 38677, USA
- ⁵¹Université de Montréal, Physique des Particules, Montréal, Québec, Canada H3C 3J7
- ⁵²Mount Holyoke College, South Hadley, Massachusetts 01075, USA
- ⁵³NIKHEF, National Institute for Nuclear Physics and High Energy Physics, NL-1009 DB Amsterdam, The Netherlands
- ⁵⁴University of Notre Dame, Notre Dame, Indiana 46556, USA
- ⁵⁵Ohio State University, Columbus, Ohio 43210, USA
- ⁵⁶University of Oregon, Eugene, Oregon 97403, USA
- ^{57a}INFN Sezione di Padova, I-35131 Padova, Italy
- ^{57b}Dipartimento di Fisica, Università di Padova, I-35131 Padova, Italy
- ⁵⁸Laboratoire de Physique Nucléaire et de Hautes Energies, IN2P3/CNRS, Université Pierre et Marie-Curie-Paris6, Université Denis Diderot-Paris7, F-75252 Paris, France
- ⁵⁹University of Pennsylvania, Philadelphia, Pennsylvania 19104, USA
- ^{60a}INFN Sezione di Perugia, I-06100 Perugia, Italy
- ^{60b}Dipartimento di Fisica, Università di Perugia, I-06100 Perugia, Italy
- ^{61a}INFN Sezione di Pisa, I-56127 Pisa, Italy
- ^{61b}Dipartimento di Fisica, Università di Pisa, I-56127 Pisa, Italy
- ^{61c}Scuola Normale Superiore di Pisa, I-56127 Pisa, Italy
- ⁶²Princeton University, Princeton, New Jersey 08544, USA
- ^{63a}INFN Sezione di Roma, I-00185 Roma, Italy
- ^{63b}Dipartimento di Fisica, Università di Roma La Sapienza, I-00185 Roma, Italy
- ⁶⁴Universität Rostock, D-18051 Rostock, Germany
- ⁶⁵Rutherford Appleton Laboratory, Chilton, Didcot, Oxon, OX11 0QX, United Kingdom
- ⁶⁶DSM/Dapnia, CEA/Saclay, F-91191 Gif-sur-Yvette, France
- ⁶⁷University of South Carolina, Columbia, South Carolina 29208, USA
- ⁶⁸Stanford Linear Accelerator Center, Stanford, California 94309, USA
- ⁶⁹Stanford University, Stanford, California 94305-4060, USA
- ⁷⁰State University of New York, Albany, New York 12222, USA
- ⁷¹University of Tennessee, Knoxville, Tennessee 37996, USA
- ⁷²University of Texas at Austin, Austin, Texas 78712, USA
- ⁷³University of Texas at Dallas, Richardson, Texas 75083, USA
- ^{74a}INFN Sezione di Torino, I-10125 Torino, Italy
- ^{74b}Dipartimento di Fisica Sperimentale, Università di Torino, I-10125 Torino, Italy
- ^{75a}INFN Sezione di Trieste, I-34127 Trieste, Italy
- ^{75b}Dipartimento di Fisica, Università di Trieste, I-34127 Trieste, Italy
- ⁷⁶IFIC, Universitat de Valencia-CSIC, E-46071 Valencia, Spain
- ⁷⁷University of Victoria, Victoria, British Columbia, Canada V8W 3P6
- ⁷⁸Department of Physics, University of Warwick, Coventry CV4 7AL, United Kingdom

⁷⁹University of Wisconsin, Madison, Wisconsin 53706, USA
(Received 16 July 2008; published 10 November 2008)

We report a study of $B^\pm \rightarrow D^* K^\pm$ decays with D^* decaying to $D\pi^0$ or $D\gamma$, using $383 \times 10^6 B\bar{B}$ pairs collected at the $Y(4S)$ resonance with the BABAR detector at the SLAC PEP-II B Factory. The D meson decays under study include a non- CP mode ($K^\pm \pi^\mp$), CP -even modes ($K^\pm K^\mp$, $\pi^\pm \pi^\mp$), and CP -odd modes ($K_S^0 \pi^0$, $K_S^0 \phi$, $K_S^0 \omega$). We measure ratios ($R_{CP^\pm}^*$) of branching fractions of decays to CP eigenmode states and to flavor-specific states as well as CP asymmetries ($A_{CP^\pm}^*$). These measurements are sensitive to the unitarity triangle angle γ . We obtain $A_{CP^+}^* = -0.11 \pm 0.09 \pm 0.01$, $R_{CP^+}^* = 1.31 \pm 0.13 \pm 0.04$, and $A_{CP^-}^* = 0.06 \pm 0.10 \pm 0.02$, $R_{CP^-}^* = 1.10 \pm 0.12 \pm 0.04$, where the first error is statistical and the second error is systematic. Translating our results into an alternative parametrization, widely used for related measurements, we obtain $x_+^* = 0.11 \pm 0.06 \pm 0.02$ and $x_-^* = 0.00 \pm 0.06 \pm 0.02$. No significant CP -violating charge asymmetry is found in either the flavor-specific mode $D \rightarrow K^\pm \pi^\mp$ or in $B^\pm \rightarrow D^* \pi^\pm$ decays.

DOI: 10.1103/PhysRevD.78.092002

PACS numbers: 14.40.Nd, 11.30.Er, 12.15.Hh, 13.25.Hw

I. INTRODUCTION

In the standard model (SM), CP -violating phenomena are a consequence of a single complex phase in the Cabibbo-Kobayashi-Maskawa (CKM) quark-mixing matrix [1]. The $B^\pm \rightarrow D^{(*)} K^{(*)\pm}$ decay modes provide a theoretically clean determination of the unitarity triangle angle γ , since the latter is equal to the relative phase between the CKM- and color-favored $b \rightarrow c$ and the CKM- and color-suppressed $b \rightarrow u$ decay amplitudes that are dominant in the considered decays. The method proposed by Gronau, London, and Wyler (GLW) makes use of the direct CP violation in the interference between the amplitudes for $B^\pm \rightarrow D^0 K^\pm$ and $B^\pm \rightarrow \bar{D}^0 K^\pm$ decays when the D^0 and \bar{D}^0 mesons decay to the same CP eigenstate [2,3]. The same approach is equally applicable when the D and/or the K meson is replaced with its excited state. In this paper we use the $B^\pm \rightarrow D^* K^\pm$ decay. We use the notation D^0 , D^{*0} , \bar{D}^0 , and \bar{D}^{*0} to denote states with definite flavor, while D_{CP^+} and $D_{CP^-}^*$ denote CP -even eigenstates, D_{CP^-} and $D_{CP^+}^*$ denote CP -odd eigenstates, and D and D^* denote any state of the $D(1864)^0$ and $D^*(2007)^0$ mesons, respectively. With the integrated luminosity presently available, it is not possible to make a precise γ measurement with the GLW method alone, but the combination of several methods and of several modes allows an improvement of the overall precision [4].

In the case of $B^\pm \rightarrow D^* K^\pm$ decays, one defines the CP -violating charge asymmetry

$$A_{CP^\pm}^* \equiv \frac{\mathcal{B}(B^- \rightarrow D_{CP^\pm}^* K^-) - \mathcal{B}(B^+ \rightarrow D_{CP^\pm}^* K^+)}{\mathcal{B}(B^- \rightarrow D_{CP^\pm}^* K^-) + \mathcal{B}(B^+ \rightarrow D_{CP^\pm}^* K^+)}, \quad (1)$$

and the ratio of branching fractions for the decays to CP eigenmodes and flavor-specific states,

$$R_{CP^\pm}^* \equiv \frac{\mathcal{B}(B^- \rightarrow D_{CP^\pm}^* K^-) + \mathcal{B}(B^+ \rightarrow D_{CP^\pm}^* K^+)}{[\mathcal{B}(B^- \rightarrow D^{*0} K^-) + \mathcal{B}(B^+ \rightarrow \bar{D}^{*0} K^+)]/2}. \quad (2)$$

We refer to the companion of the charmed meson in the final state as the prompt track. Experimentally, it is convenient to normalize the branching fractions of the decays with a prompt kaon in the final state to those of the similar decays with a prompt pion that have a larger branching fraction. The ratio $R_{CP^\pm}^*$ can then be expressed as

$$R_{CP^\pm}^* \approx \frac{R_\pm^*}{R^*}, \quad (3)$$

where R_\pm^* and R^* are the K/π ratios

$$R_\pm^* \equiv \frac{\mathcal{B}(B^- \rightarrow D_{CP^\pm}^* K^-) + \mathcal{B}(B^+ \rightarrow D_{CP^\pm}^* K^+)}{\mathcal{B}(B^- \rightarrow D_{CP^\pm}^* \pi^-) + \mathcal{B}(B^+ \rightarrow D_{CP^\pm}^* \pi^+)} \quad (4)$$

and

$$R^* \equiv \frac{\mathcal{B}(B^- \rightarrow D^{*0} K^-) + \mathcal{B}(B^+ \rightarrow \bar{D}^{*0} K^+)}{\mathcal{B}(B^- \rightarrow D^{*0} \pi^-) + \mathcal{B}(B^+ \rightarrow \bar{D}^{*0} \pi^+)}. \quad (5)$$

The ratio R^* is predicted to be of the order of $[(f_K/f_\pi) \times |V_{us}/V_{ud}|]^2 = 0.080 \pm 0.002$ [5], where f_K and f_π are the form factors of the mesons. Equation (3) would be an equality if CP violation was completely absent in $B \rightarrow D^* \pi$ decays. Defining the charge asymmetry

$$A_h^* \equiv \frac{\mathcal{B}(B^- \rightarrow D^* h^-) - \mathcal{B}(B^+ \rightarrow D^* h^+)}{\mathcal{B}(B^- \rightarrow D^* h^-) + \mathcal{B}(B^+ \rightarrow D^* h^+)} \quad (6)$$

(noted A_π^* and A_K^* when referring to $h = \pi$ and $h = K$, respectively), this approximation implies that the pion charge asymmetry A_π^* should be compatible with zero, as

*Deceased.

[†]Now at Temple University, Philadelphia, PA 19122, USA.

[‡]Now at Tel Aviv University, Tel Aviv, 69978, Israel.

[§]Also with Università di Perugia, Dipartimento di Fisica, Perugia, Italy.

^{||}Also with Università di Roma La Sapienza, I-00185 Roma, Italy.

[¶]Now at University of South Alabama, Mobile, AL 36688, USA.

^{**}Also with Università di Sassari, Sassari, Italy.

should be the kaon charge asymmetry A_K^* for the flavor-specific modes $D \rightarrow K^\pm \pi^\mp$. The possible bias induced by this approximation is expected to be small since the ratio of the amplitudes of the $B^- \rightarrow \bar{D}^{*0} \pi^-$ and $B^- \rightarrow D^{*0} \pi^-$ processes is predicted to be of the order of 1% [6] in the SM, and will be accounted for in the systematic uncertainties.

Most experimental systematic uncertainties, such as those related to the reconstruction of the D^* , and the uncertainties on the D decay branching fractions, cancel in the K/π ratios R^* and R_{\pm}^* . By neglecting the small [7,8] D^0 - \bar{D}^0 mixing [9] and CP violation in D^0 decays, $R_{CP\pm}^*$ and $A_{CP\pm}^*$ are related to γ through

$$R_{CP\pm}^* = 1 + r_B^{*2} \pm 2r_B^* \cos\delta_B^* \cos\gamma \quad (7)$$

and

$$A_{CP\pm}^* = \frac{\pm 2r_B^* \sin\delta_B^* \sin\gamma}{1 + r_B^{*2} \pm 2r_B^* \cos\delta_B^* \cos\gamma}, \quad (8)$$

where r_B^* is the magnitude of the ratio of the amplitudes for the processes $B^- \rightarrow \bar{D}^{*0} K^-$ and $B^- \rightarrow D^{*0} K^-$, and δ_B^* is the relative strong phase between these two amplitudes. The ratio r_B^* involves a CKM factor $|V_{ub}V_{cs}/V_{cb}V_{us}| \approx 0.44 \pm 0.05$ [5] and a color suppression factor that has been estimated to lie between $0.26 \pm 0.07 \pm 0.05$ [10] and 0.44 [6], so that r_B^* is predicted to be in the range 0.1–0.2. More recent calculations that take into account final state interactions [11] yield predictions of $r_B^* = 0.09 \pm 0.02$.

The latest results by *BABAR* and *Belle* are reported in Refs. [12–14], respectively. *BABAR* used $123 \times 10^6 B\bar{B}$ pairs with $D^* \rightarrow D\pi^0$ and D reconstructed in the CP -even modes K^+K^- and $\pi^+\pi^-$, and non- CP modes $K^\pm\pi^\mp$, $K^\pm\pi^-\pi^+\pi^\mp$, and $K^\pm\pi^\mp\pi^0$. *Belle* used $275 \times 10^6 B\bar{B}$ pairs with $D^* \rightarrow D\pi^0$ and D reconstructed in the CP -even modes K^+K^- and $\pi^+\pi^-$, CP -odd modes $K_S^0\pi^0$, $K_S^0\omega$, $K_S^0\phi$, and non- CP modes $K^\pm\pi^\mp$ [13]. The results are summarized in Table I. Similar studies have been performed on the channels $B^\pm \rightarrow DK^\pm$ [13,15,16] and $B^\pm \rightarrow DK^{*\pm}$ [17].

The *BABAR* [18] and *Belle* [19] experiments have recently obtained estimates of r_B^* and δ_B^* parameters from the overlap of the D^0 and \bar{D}^0 decays in the Dalitz planes of some three-body D decays. *BABAR* obtains $r_B^* = 0.135 \pm 0.051$ and $\delta_B^* = (-63_{-30}^{+28})^\circ$, while *Belle* obtains $r_B^* = 0.21 \pm 0.08 \pm 0.02 \pm 0.05$ and $\delta_B^* = (342_{-23}^{+21} \pm 4 \pm 23)^\circ$ (where the first error is statistical, the second is the experi-

mental systematic uncertainty, and the third reflects the uncertainty on the D decay Dalitz models).

In this paper, by using $(383 \pm 4) \times 10^6 B\bar{B}$ pairs, we update the results of our previous study of $B^\pm \rightarrow D^*K^\pm$ decays [12] for D decays to the CP -even modes K^+K^- , $\pi^+\pi^-$ and to the flavor-specific modes $K^\pm\pi^\mp$, and we extend it to the CP -odd modes $K_S^0\pi^0$, $K_S^0\omega$, and $K_S^0\phi$, and to $D^* \rightarrow D\gamma$. Because of parity and angular-momentum conservation, the CP eigenvalue of the D^* is inferred from that of the D , when the CP eigenvalue of the neutral companion (γ or π^0) is taken into account [20]: $CP(D^*) = CP(D)$ when $D^* \rightarrow D\pi^0$, and $CP(D^*) = -CP(D)$ when $D^* \rightarrow D\gamma$.

Experimental results can also be presented using the ‘‘Cartesian coordinates’’

$$(x_\pm^*, y_\pm^*) \equiv (r_B^* \cos(\delta_B^* \pm \gamma), r_B^* \sin(\delta_B^* \pm \gamma)), \quad (9)$$

which have the advantage of having Gaussian uncertainties, and of being uncorrelated and unbiased (r_B^* , being positive, is biased towards larger values in low precision measurements, whereas x_\pm^* and y_\pm^* show no such bias) [21]. The parameters x_\pm^* can be obtained from $R_{CP\pm}^*$ and $A_{CP\pm}^*$,

$$x_\pm^* = \frac{R_{CP+}^*(1 \mp A_{CP+}^*) - R_{CP-}^*(1 \mp A_{CP-}^*)}{4}. \quad (10)$$

The measurements presented in this paper have no direct sensitivity to y_\pm^* , in contrast to Dalitz analyses. However, an indirect constraint can be obtained using

$$(r_B^*)^2 = x_\pm^{*2} + y_\pm^{*2} = \frac{R_{CP+}^* + R_{CP-}^* - 2}{2}. \quad (11)$$

Note that there are four observables in these parametrizations, either $(A_{CP+}^*, R_{CP+}^*, A_{CP-}^*, R_{CP-}^*)$ or $(x_+^*, y_+^*, x_-^*, y_-^*)$, while there are only three independent fundamental parameters, $(\gamma, r_B^*, \delta_B^*)$. The set of parameters must therefore fulfill one constraint, which can be $\kappa = 0$, where

$$\kappa \equiv R_{CP+}^* A_{CP+}^* + A_{CP-}^* R_{CP-}^*. \quad (12)$$

II. THE DATA SET AND DETECTOR

The results presented in this paper are based on data collected with the *BABAR* detector at the PEP-II asymmetric-energy e^+e^- storage ring of the Stanford Linear Accelerator Center. At PEP-II, 9.0 GeV electrons and 3.1 GeV positrons collide at a center-of-mass energy of 10.58 GeV, which corresponds to the mass of the $Y(4S)$

TABLE I. Past measurements of parameters related to the measurement of γ in $B^\pm \rightarrow D^*K^\pm$ decays by the GLW method.

	A_{CP+}^*	A_{CP-}^*	R_{CP+}^*	R_{CP-}^*	R^*
<i>BABAR</i> [12]	$-0.10 \pm 0.23_{-0.04}^{+0.03}$...	$1.06 \pm 0.26_{-0.09}^{+0.10}$...	$0.0813 \pm 0.0040_{-0.0031}^{+0.0042}$
<i>Belle</i> [13,14]	$-0.20 \pm 0.22 \pm 0.04$	$0.13 \pm 0.30 \pm 0.08$	$1.41 \pm 0.25 \pm 0.06$	$1.15 \pm 0.31 \pm 0.12$	$0.078 \pm 0.019 \pm 0.009$

resonance. The asymmetric beam energies result in a boost from the laboratory to the center-of-mass frame of $\beta\gamma \approx 0.56$. The data set analyzed in this paper corresponds to an integrated luminosity of 347 fb^{-1} at the $Y(4S)$ resonance.

The *BABAR* detector is described in detail elsewhere [22]. Surrounding the interaction point is a five-layer double-sided silicon vertex tracker (SVT), which measures the trajectories of charged particles. A 40-layer drift chamber (DCH) provides measurements of the momenta of charged particles. Both the SVT and DCH are located inside a 1.5 T magnetic field provided by a solenoid magnet. Charged hadron identification is achieved through measurements of particle energy loss in the tracking system and the Cherenkov angle obtained from a detector of internally reflected Cherenkov light (DIRC). A CsI(Tl) electromagnetic calorimeter (EMC) provides photon detection, electron identification, and π^0 reconstruction. Finally, the instrumented flux return (IFR) of the magnet enables discrimination of muons from pions. For the most recent 134 fb^{-1} of data, a fraction of the resistive plate chambers constituting the muon system has been replaced by limited streamer tubes [23].

We use Monte Carlo (MC) simulation to study the detector acceptance and backgrounds. The MC simulation uses the EVTGEN generator [24] and GEANT4 [25] to simulate the passage of particles through matter.

III. RECONSTRUCTION OF B CANDIDATES

We perform an exclusive reconstruction of the full B meson decay chain, in the modes described in the Introduction, starting from the final stable products (charged-particle tracks and neutral electromagnetic deposits in the EMC).

The π^0 candidates used to form an ω , a D , or a D^* candidate are reconstructed from pairs of photons with energies larger than 30 MeV, and shower shapes consistent with electromagnetic showers, with invariant mass in the range $115 < m_{\gamma\gamma} < 150 \text{ MeV}/c^2$. In addition, the π^0 candidates used to form a D^* candidate are required to have center-of-mass frame momenta $p_{\gamma\gamma}^* < 450 \text{ MeV}/c$. The ω candidates are reconstructed in the three-body decay $\omega \rightarrow \pi^+ \pi^- \pi^0$, with an invariant mass within $50 \text{ MeV}/c^2$ of the world average [5]. We reconstruct $K_S^0 \rightarrow \pi^+ \pi^-$ candidates from pairs of oppositely charged tracks that are consistent with having originated from a common vertex position and with an invariant mass within $25 \text{ MeV}/c^2$ of the world average [5]. We reconstruct $\phi \rightarrow K^+ K^-$ candidates from pairs of oppositely charged tracks with particle identification inconsistent with a pion hypothesis, that are consistent with having originated from a common vertex position, and that have invariant mass within $30 \text{ MeV}/c^2$ of the world average [5].

Only two-body D decays are considered in this study. The D candidates are reconstructed from their two daugh-

ters that are required to be consistent with having originated from a common vertex position. In the case of $D \rightarrow K_S^0 \pi^0$, in which vertexing of the $K_S^0 \pi^0$ system would yield a poor geometrical constraint, a beam spot constraint is added to the fit in order to force the D daughters to originate from the interaction region.

The D^* candidates are formed from D and π^0 or γ candidates. These photon candidates are required to have energies larger than 100 MeV and shower shapes consistent with electromagnetic showers. The D^* candidates are required to fulfill $130 < \Delta m < 170 \text{ MeV}/c^2$ and $80 < \Delta m < 180 \text{ MeV}/c^2$, respectively, where Δm is the invariant mass difference between the D^* and the D candidate.

The π^0 , K_S^0 , D , and D^* candidates are refitted with mass constraints before their four-momenta are used to reconstruct the B decay chain. We form B candidates from D^* candidates and charged tracks, fitted with a beam spot constraint. We characterize B candidates by two kinematic variables: the difference between the reconstructed energy of the B candidate and the beam energy in the center-of-mass frame $\Delta E_K \equiv E_B^* - \sqrt{s}/2$, and the beam-energy substituted mass $m_{\text{ES}} \equiv \sqrt{(s/2 + \mathbf{p}_0 \cdot \mathbf{p}_B)^2/E_0^2 - \mathbf{p}_B^2}$, where (E_0, \mathbf{p}_0) and (E_B, \mathbf{p}_B) are the four-momenta of the $Y(4S)$ and B meson candidate, respectively, the asterisk denotes the $Y(4S)$ rest frame, and \sqrt{s} is the total energy in the $Y(4S)$ rest frame. The subscript K in ΔE_K indicates that the kaon hypothesis has been assumed for the prompt track in the computation of ΔE . For a correctly reconstructed B meson having decayed to a D^*K final state, ΔE_K is expected to peak near zero, with an R.M.S. of about 16 MeV, and m_{ES} is expected to peak near the B meson mass $5.279 \text{ GeV}/c^2$, with an R.M.S. that is almost independent of the channel and close to $3 \text{ MeV}/c^2$. For a $B \rightarrow D^*\pi$ decay reconstructed as $B \rightarrow D^*K$ with a correctly identified D^* , the ΔE_K peak is shifted by approximately +50 MeV. At reconstruction level, the loose requirements $5.2 < m_{\text{ES}} < 5.3 \text{ GeV}/c^2$ and $|\Delta E_K| < 0.2 \text{ GeV}$ are applied to the B meson candidate.

We form a Fisher discriminant \mathcal{F} [26] to distinguish signal events from the significant background due to $e^+e^- \rightarrow q\bar{q}$ ($q = u, d, s, c$) continuum events. Six variables are used:

- (i) L_0 and L_2 , the zeroth and second angular moments of the energy flow around the B thrust axis. They are defined as $\sum_i p_i$ and $\sum_i p_i \cos^2 \theta_i$, respectively, where p_i is the momentum and θ_i is the angle with respect to the thrust axis of the B candidate, both in the center-of-mass frame, for all tracks and neutral clusters not used to reconstruct the B meson.
- (ii) R_2 , the ratio of the second to the zeroth Fox-Wolfram moment [27] of charged tracks and neutral clusters in the center-of-mass frame.
- (iii) $|\cos \theta_B|$, where θ_B is the angle between the momentum of the B candidate and the boost direction of the e^+e^- center-of-mass frame.

- (iv) $|\cos\theta_{\text{Thrust}}|$, where θ_{Thrust} is the angle between the B candidate thrust vector and the beam axis in the center-of-mass frame.
- (v) $|\cos\theta_{\text{T}}|$, where θ_{T} is the angle between the B candidate thrust axis and the thrust axis of the rest of the event in the center-of-mass frame (where the rest of the event corresponds to reconstructed particles not associated with the B candidate).

IV. SELECTION OF B CANDIDATES

After the preliminary event reconstruction, a large amount of background remains in the signal candidate sample. In this section we describe the additional selection criteria used to reduce the background.

The selection of each $B \rightarrow D^*K$ decay mode is optimized separately, by the maximization of the sensitivity $S/\sqrt{S+B+1}$, where $\sqrt{S+B+1}$ is a symmetrized approximation of the Poisson uncertainty on the measurement of $S+B$. The numbers S and B of signal and background expected events are estimated from, respectively, high-statistics exclusive MC samples, and a cocktail of generic B^+B^- (with signal events removed), $B^0\bar{B}^0$, and $q\bar{q}$ MC samples.

In the optimization procedure, we include requirements on all variables, including those that will be relaxed during the fit, and including tightening requirements that have been made in the reconstruction stage. Our optimization procedure is similar to that used in Ref. [28], and allows us to determine the optimal set of variables as well as the optimal requirements on those variables, by the examination of the signal-to-background ratio distributions [29]. The final set of variables on which we apply selection optimization is as follows:

- (i) The B candidate-related variables m_{ES} and ΔE_K introduced above.
- (ii) The mass m_{D^0} of the D candidate before the mass constraint is applied, and the mass difference Δm .
- (iii) Likelihood ratios for the prompt track that are evaluated making use of the Cherenkov angle information from the DIRC, and of the dE/dx information provided by the tracking system. Explicitly, we compute likelihoods \mathcal{L}_h for particle identification (PID) hypotheses $h = K, \pi, p$ and make requirements on the ratios $\mathcal{L}_K/(\mathcal{L}_K + \mathcal{L}_\pi)$ and $\mathcal{L}_K/(\mathcal{L}_K + \mathcal{L}_p)$. We also require that the track is not identified as an electron or a muon.
- (iv) Likelihood ratios for pion and kaon candidates that are daughters of two-body D decays.
- (v) The value of the Fisher variable \mathcal{F} .
- (vi) The invariant masses of the K_S^0, ϕ, π^0 , and ω candidates, when relevant, and before the mass constraints. Furthermore, for decays involving K_S^0 candidates, we include the ratio of the flight length of K_S^0 candidates in the transverse plane divided by its uncertainty, and require it to be larger than 2.

For decays involving ω candidates, we include $|\cos(\theta_\omega)|$, where θ_ω is the angle between the normal to the pion decay plane and the D direction in the ω rest frame.

The selection requirements applied to these variables are mode dependent, except for the prompt-track PID requirements $\mathcal{L}_K/(\mathcal{L}_K + \mathcal{L}_\pi) > 0.9$ and $\mathcal{L}_K/(\mathcal{L}_K + \mathcal{L}_p) > 0.2$ that are applied to all $B \rightarrow D^*K$ channels. The selection of the $B^\pm \rightarrow D^*\pi^\pm$ modes is identical to that of the $B^\pm \rightarrow D^*K^\pm$ modes, except for the prompt-track PID that is reversed [$\mathcal{L}_K/(\mathcal{L}_K + \mathcal{L}_\pi) < 0.2$].

A fraction of the events have several B candidates selected: the average multiplicity varies from 1.07 to 1.66 for $D^* \rightarrow D\pi^0$ and from 1.00 to 1.25 for $D^* \rightarrow D\gamma$, depending on the channel. We select the B candidate that has the B vertex fit with the largest probability. This best-candidate procedure is used during the optimization of the selection that we have described above. The probability of selection of the well-reconstructed signal candidate is mode dependent and is in the range 56%–72% for $D^* \rightarrow D\pi^0$ decays and in the range 68%–81% for $D^* \rightarrow D\gamma$ decays.

V. MAXIMUM LIKELIHOOD FIT

The dominant contribution to the remaining background after event selection is from B decays, including a significant amount of feed-across from $B^\pm \rightarrow D^*\pi^\pm$ decays. Therefore the measurement is performed with an unbinned likelihood fit [30,31] based on two variables that best discriminate this background, namely, ΔE_K and a PID variable $\mathcal{T}_{\mathcal{R}}$ defined below.

As the prompt-track PID likelihood ratio $\mathcal{R} \equiv \mathcal{L}_K/(\mathcal{L}_K + \mathcal{L}_\pi)$ is very strongly peaked near zero for pions and near 1 for kaons, we use a pseudologarithmic change of variable

$$\mathcal{T}_{\mathcal{R}} = \log_{10}\left(\frac{\mathcal{R} + \epsilon}{1 - \mathcal{R} + \epsilon}\right). \quad (13)$$

We include a small positive number $\epsilon = 10^{-7}$, so that $\mathcal{T}_{\mathcal{R}}$ is always defined, with $\mathcal{T}_{\mathcal{R}} = +7$ for $\mathcal{R} = 1$ (“perfect kaons”) and $\mathcal{T}_{\mathcal{R}} = -7$ for $\mathcal{R} = 0$ (“perfect pions”).

The measurement is performed with an extended unbinned maximum likelihood function

$$\mathcal{L} = \frac{e^{-N'}(N')^N}{N!} \prod_{i=1}^N \mathcal{P}_i, \quad (14)$$

where N is the number of events in the sample to fit, N' is the expected number, and for event i

$$\mathcal{P}_i = \frac{1}{N'} \sum_j N_j \mathcal{P}_i^j, \quad (15)$$

where $j = D^*K, D^*\pi, B_K, B_\pi$ is one of four event categories: signal kaon and pion, and background kaon and pion, respectively, where the background is a combination

of continuum, B^+B^- , and $B^0\bar{B}^0$ events. The quantity \mathcal{P}_i^j is the probability density function (PDF) for event i and category j , and N_j is the number of events in category j .

For the signal categories, the distance between the kaon and pion ΔE_K peaks provides powerful separation between pions and kaons, in addition to PID. For the background categories, we use mutually exclusive likelihood-based pion and kaon selectors, that, in particular, contain requirements of $\mathcal{R} > 0.9$ (kaon) and $\mathcal{R} < 0.1$ (pion), respectively. For consistency and symmetry reasons, the whole region $0.1 < \mathcal{R} < 0.9$ is removed for all categories, including the signal categories used in the fit.

The correlations between \mathcal{T}_R and ΔE_K are found to be small (compatible with zero for the signal K and for the background categories, and with -6% for the π signal category); therefore, a factorized approximation is used:

$$\mathcal{P}_i^j(\Delta E_K, \mathcal{T}_R) = \mathcal{P}_i^j(\Delta E_K)\mathcal{P}_i^j(\mathcal{T}_R). \quad (16)$$

We have checked that no bias is introduced by this approximation by simulating a large number of experiments in which the signal is taken from the large statistics exclusive MC samples used for estimating these correlations.

The PDFs used in the fit are determined from MC samples. The signal ΔE_K PDFs are parametrized with double Gaussian functions. The background PDFs are mode-dependent functions chosen to best represent the MC background distributions: they include Gaussian, exponential, and third-order Chebyshev polynomial functions. The complicated shape of the ΔE_K distribution of the B_π category arises from the contributions from several distinct components: at low ΔE_K values, $B^\pm \rightarrow D^*\rho^\pm$ decays dominate; in the signal region, the background is mainly composed of $\gamma \leftrightarrow \pi^0$ cross feed and of $B^\pm \rightarrow D^0\pi^\pm$, the latter of which dominates at high ΔE_K values. The \mathcal{T}_R

PDFs are histograms, determined from MC samples, with a binning $\Delta\mathcal{T}_R = 0.5$ and, therefore, 28 bins. MC-based studies have shown that the results of such fits do not depend on the number of bins n_b as long as $n_b > 2$.

We correct for a small discrepancy in PID efficiencies between data and MC samples, using high-statistics high-purity kaon and pion samples from inclusive $D^{*\pm} \rightarrow D\pi^\pm$, $D \rightarrow K^\pm\pi^\mp$ data. The difference in track momentum spectra between these control samples and the exclusive modes studied in the present analysis is accounted for in the correction procedure. This is achieved by weighting the control sample \mathcal{T}_R PDF by the ratio of the MC to control sample prompt-track momentum distributions for both cases of the prompt track being a kaon or a pion. An example of the PDFs used for the channel $D^* \rightarrow D\pi^0$, $D \rightarrow K^\pm\pi^\mp$ is shown in Fig. 1.

For signal events with a pion prompt track, for which ΔE_π (the subscript π indicates that the pion hypothesis has been assumed for the prompt track in the computation of ΔE) is close to zero, the relation

$$\Delta E_K - \Delta E_\pi \approx \frac{1}{2p} \frac{E_{Y(4S)}}{m_{Y(4S)}} (m_K^2 - m_\pi^2) \quad (17)$$

introduces a mild dependence of ΔE_K on the momentum p of the prompt track. The parameters $E_{Y(4S)}$ and $m_{Y(4S)}$, m_K , m_π denote the energy of the e^+e^- system in the laboratory frame and the masses of the mesons, respectively. Fits taking this dependence into account do not show any significant improvement, nor degradation.

Fits performed on the B^+B^- , $B^0\bar{B}^0$, and $q\bar{q}$ background MC samples show no significant bias. Similar fits with either pion or kaon signal events removed yield numbers of signal events compatible with zero for the removed category. This indicates that the factorization approxima-

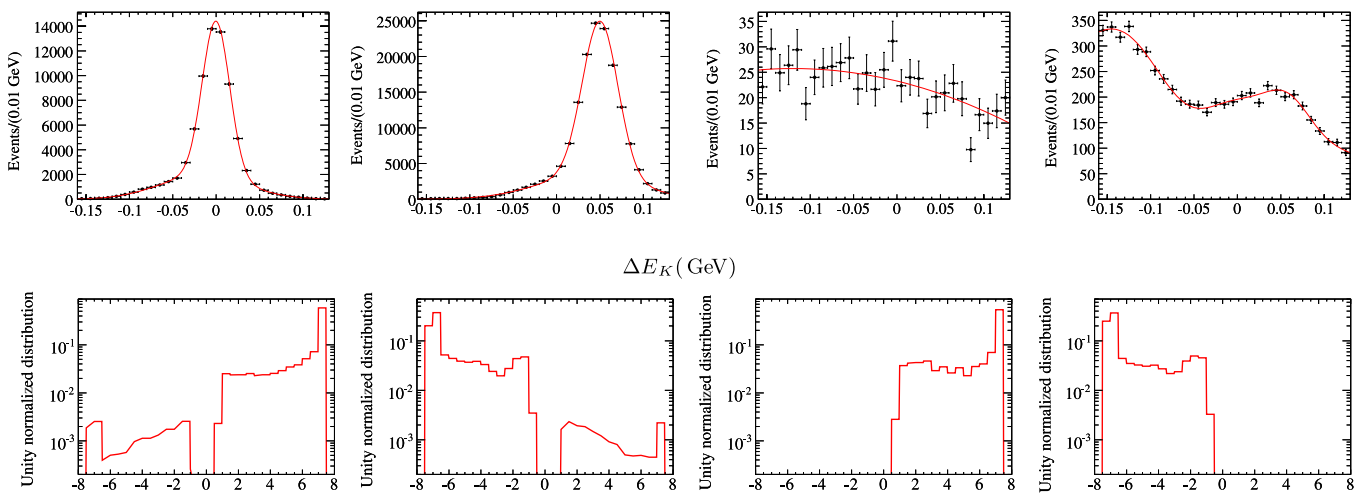


FIG. 1 (color online). Distributions of ΔE_K (upper plots) and the PID variable \mathcal{T}_R (lower plots) from MC simulations of the categories (from left to right) D^*K , $D^*\pi$, B_K , and B_π (the latter two from B^+B^- , $B^0\bar{B}^0$, and $q\bar{q}$ MC samples), for the mode $D^* \rightarrow D\pi^0$, $D \rightarrow K^\pm\pi^\mp$. In the upper plots, the dots represent the MC sample spectrum, and the curves show the PDFs. Note the vertical log scale in the lower plots.

TABLE II. Selection efficiencies (in %) for channels used in this analysis for each decay mode of the D (statistical uncertainties only).

	$(D\pi^0)K^\pm$	$(D\gamma)K^\pm$	$(D\pi^0)\pi^\pm$	$(D\gamma)\pi^\pm$ (in %)
$K^\pm\pi^\mp$	21.0 ± 0.1	24.7 ± 0.1	22.2 ± 0.1	24.9 ± 0.1
$\pi\pi$	14.6 ± 0.1	14.7 ± 0.1	14.8 ± 0.1	14.8 ± 0.1
KK	20.4 ± 0.1	21.1 ± 0.1	20.5 ± 0.1	21.2 ± 0.1
$K_S^0\pi^0$	8.9 ± 0.1	8.8 ± 0.1	8.9 ± 0.1	9.0 ± 0.1
$K_S^0\omega$	4.4 ± 0.1	4.2 ± 0.1	4.5 ± 0.1	4.3 ± 0.1
$K_S^0\phi$	10.3 ± 0.1	13.5 ± 0.1	10.4 ± 0.1	13.7 ± 0.1

tion made for the background PDF does not create any bias on the number of fitted signal events.

Signal efficiencies are estimated from fits on high-statistics exclusive MC samples and summarized in Table II. We perform separate fits for each D^* decay mode, and subsequently perform a weighted average to obtain our final results for $R_{CP^\pm}^*$ and $A_{CP^\pm}^*$. The free parameters of each fit are itemized here:

- (i) the charge-averaged K/π ratio (one parameter, R_\pm^* or R^* , whenever relevant);
- (ii) the number of pion signal events (one parameter);
- (iii) the pion and kaon charge asymmetries A_h^* of the signal (two parameters);
- (iv) the number of pion and kaon background events, and charge asymmetries (four parameters);
- (v) the position of the ΔE_K peak of the pion events (one parameter).

In total there are nine free parameters for each D^* mode.

VI. SYSTEMATIC UNCERTAINTIES

The systematic uncertainties are summarized in Table III.

The contribution of the determination of the ΔE_K signal PDFs to the systematic uncertainty is estimated by varying the parameters that are fixed in the fit by 1 standard deviation ($\pm 1\sigma$). The contribution of the ΔE_K PDFs of the B_K category for the $D^{*0} \rightarrow D\pi^0$ decays is determined similarly.

For the other ΔE_K background PDFs, this approach cannot be used, as the correlations between parameters are not small. The contribution to the systematics due to the limited MC statistics used to determine the parameters of the PDFs is obtained in the following way. We determine two separate parametrizations of the PDFs on two halves of the MC sample, and perform the fits with them. We take half the difference between the obtained results as an estimate of the systematics.

The contribution of the determination of the \mathcal{T}_R signal PDFs to the systematic uncertainty is estimated by performing an additional fit without the correction of the small discrepancy between data and MC samples described

above. The difference between the results of both fits is taken as an estimate of the uncertainty.

The systematic uncertainty introduced by the limited knowledge of $B^\pm \rightarrow D^*\rho^\pm$ and $B^0 \rightarrow D^{*+}\pi^-$ branching fractions is estimated from MC samples by performing a fit on a sample in which the number of these events is varied by $\pm 1\sigma$ [5].

Differences in the interactions of positively and negatively charged kaons with the detector and the possible charge asymmetry of the detector are studied using the exclusive MC samples. Asymmetries of $(-1.0 \pm 0.2)\%$ and $(0.2 \pm 0.2)\%$ are observed for kaon and pion modes, respectively, for the CP modes. A correction of $+1\%$ is applied to the measured values of A_{CP}^* . The simulation of the detector charge asymmetry has been compared to the actual value in the data in a previous analysis of B decays to $K\pi$ [32]. The possible discrepancy has been found to be smaller than 1% .

The $\pi^0 \leftrightarrow \gamma$ cross feed can reduce the value of $A_{CP^\pm}^*$ because, for a given D_{CP} final state, D_{CP}^* has the same CP value as D_{CP} if decaying to $D\pi^0$ and the opposite CP value if decaying to $D\gamma$ [20]. This “ CP dilution” is estimated from MC samples by performing a fit in which the potential feed-across has been completely removed. The effect is similar among modes and is accounted for by an uncertainty of 0.5% for $D\pi^0$ modes and of 1.0% for $D\gamma$ modes.

In the case of D decays to $K_S^0\phi$ and $K_S^0\omega$, the CP -violating charge asymmetry can be diluted by the presence of decays to the same final state that may have a different CP composition ($K_S^0K^+K^-$ and $K_S^0\pi^+\pi^-\pi^0$, respectively). This S -wave effect is accounted for in a way similar to that used in our previous study of the DK modes [15]. It consists of applying a correction to the measured $A_{CP^\pm}^*$ and $R_{CP^\pm}^*$ values using the CP content information of $K_S^0K^+K^-$ and $K_S^0\pi^+\pi^-\pi^0$ modes. The uncertainty on the correcting factors is then propagated to the correction formula and included as an additional systematic uncertainty on $A_{CP^\pm}^*$ and $R_{CP^\pm}^*$.

The correlations between the different sources of systematic errors are negligible and neglected when combining the two CP -even or the three CP -odd modes.

No systematic error or correction is applied to account for selection efficiency uncertainties, as we do not measure

TABLE III. Contributions to systematic uncertainties for each mode on the measurement of the charge asymmetries A_K^* , and the ratio R_{CP}^* of CP eigenmode to flavor-specific mode (10^{-3}). See text for details.

$D^* \rightarrow D\pi^0$							
A_K^*		$K\pi$	$\pi\pi$	KK	$K_S^0\pi^0$	$K_S^0\omega$	$K_S^0\phi$ (10^{-3})
	ΔE_K	0	22	5	9	6	10
	$\mathcal{T}_{\mathcal{R}}$	1	12	2	18	22	38
	$\mathcal{B}(D^*\rho^-)$	3	4	0	1	2	59
	$\mathcal{B}(D^{*-}\pi^+)$	1	1	1	1	6	0
	$\pi^0 \leftrightarrow \gamma$	0	5	5	5	5	5
	S-wave	33	2
	Total	3	26	7	21	41	71
R_{CP}^*							
		$K\pi$	$\pi\pi$	KK	$K_S^0\pi^0$	$K_S^0\omega$	$K_S^0\phi$ (10^{-3})
	ΔE_K	...	80	34	54	116	54
	$\mathcal{T}_{\mathcal{R}}$...	16	13	10	32	6
	$\mathcal{B}(D^*\rho^-)$...	51	22	14	5	131
	$\mathcal{B}(D^{*-}\pi^+)$...	3	5	1	21	4
	S-wave	141	40
	Total	...	96	42	57	187	147
$D^* \rightarrow D\gamma$							
A_K^*		$K\pi$	$\pi\pi$	KK	$K_S^0\pi^0$	$K_S^0\omega$	$K_S^0\phi$ (10^{-3})
	ΔE_K	1	39	8	19	66	52
	$\mathcal{T}_{\mathcal{R}}$	16	4	39	18	75	22
	$\mathcal{B}(D^*\rho^-)$	4	1	0	1	18	1
	$\mathcal{B}(D^{*-}\pi^+)$	4	3	4	0	18	3
	$\pi^0 \leftrightarrow \gamma$	0	10	10	10	10	10
	S-wave	40	5
	Total	17	40	41	28	111	58
R_{CP}^*							
		$K\pi$	$\pi\pi$	KK	$K_S^0\pi^0$	$K_S^0\omega$	$K_S^0\phi$ (10^{-3})
	ΔE_K	...	136	59	64	393	230
	$\mathcal{T}_{\mathcal{R}}$...	17	34	4	78	42
	$\mathcal{B}(D^*\rho^-)$...	1	2	12	5	23
	$\mathcal{B}(D^{*-}\pi^+)$...	11	9	3	13	8
	S-wave	192	47
	Total	...	138	69	65	445	239

branching fractions but ratios of branching fractions in which they largely cancel.

For the branching fraction ratios $R_{CP\pm}^*$, in addition to the sources of systematic uncertainties listed in Table III, we associate one more uncertainty with the assumption that $R_{CP\pm}^* = R_{\pm}^*/R^*$. This assumption holds only if the magnitude of the ratio r_{π}^* between the amplitudes of the $B^- \rightarrow \bar{D}^{*0}\pi^-$ and $B^- \rightarrow D^{*0}\pi^-$ processes is neglected [6]. The ratio r_{π}^* is expected to be small: $r_{\pi}^* \sim r_B^* \frac{\lambda^2}{1-\lambda^2}$, where $\lambda \approx 0.22$ [5] is the sine of the Cabibbo angle. This introduces a relative uncertainty of $\pm 2r_{\pi}^* \cos\delta_{\pi}^* \cos\gamma$ on $R_{CP\pm}^*$, where δ_{π}^* is the relative strong phase between $\mathcal{A}(B^- \rightarrow \bar{D}^{*0}\pi^-)$ and $\mathcal{A}(B^- \rightarrow D^{*0}\pi^-)$. Since $|\cos\delta_{\pi}^* \cos\gamma| \leq 1$ and $r_{\pi}^* \leq 0.007$, we assign a relative uncertainty of $\pm 1.4\%$ to $R_{CP\pm}^*$,

which is completely anticorrelated between R_{CP+}^* and R_{CP-}^* .

VII. RESULTS

We plot the ΔE_K distributions in Fig. 2 with a kaon selection ($\mathcal{T}_{\mathcal{R}} > 0$) applied, and with the fitted PDFs overlaid. The results are summarized in Table IV, with the observed numbers of charged-averaged events in Table V. Note that none of the corrections between data and MC samples that would be needed for measurements of absolute branching fractions are used here, as we are interested in ratios only. We have checked that charge asymmetries of $B^{\pm} \rightarrow D^* \pi^{\pm}$ modes are compatible with zero as

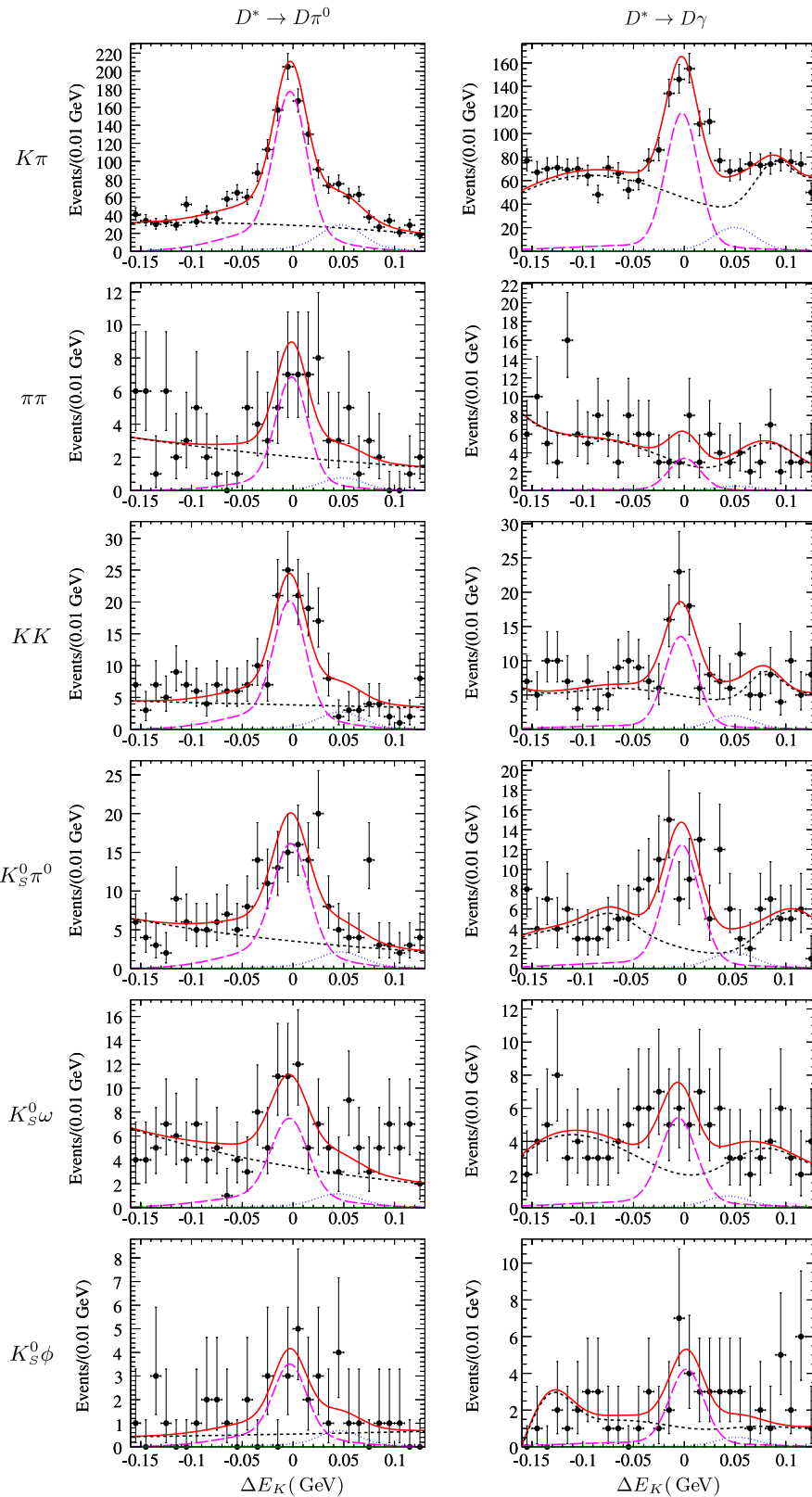


FIG. 2 (color online). ΔE_K distributions, with a cut on the PID variable $\mathcal{T}_R > 0$ to enhance the kaon part of the sample. Distributions are shown for each of the decays modes: (left panels) $D^* \rightarrow D\pi^0$ and (right panels) $D^* \rightarrow D\gamma$, with the D decay modes indicated on the left of the figure. Dots denote the distribution of the data. Curves denote the PDFs for the various categories: signal K (long-dashed curve), signal π (dotted curve), and background K (short-dashed curve); background π does not appear because the $\mathcal{T}_R > 0$ cut completely removes this category. The thick curve denotes the total PDF.

TABLE IV. Summary of measurements of the charge asymmetries A_K^* ; the CP eigenmode to flavor-specific mode ratios R_{CP}^* ; and the Cartesian parameters x^* , for B^\pm decays to CP -even and CP -odd eigenmodes $D_{CP}^* K^\pm$. The value of A_K^* for the flavor-specific control mode with $D \rightarrow K^\pm \pi^\mp$ is also given.

	A_K^*	R_{CP}^*	x^*
Flavor specific	$-0.06 \pm 0.04 \pm 0.01$
$CP+$	$-0.11 \pm 0.09 \pm 0.01$	$1.31 \pm 0.13 \pm 0.04$	$0.11 \pm 0.06 \pm 0.02$
$CP-$	$0.06 \pm 0.10 \pm 0.02$	$1.10 \pm 0.12 \pm 0.04$	$0.00 \pm 0.06 \pm 0.02$

TABLE V. Number of events measured in this analysis (statistical uncertainties only).

	$(D\pi^0)K^\pm$	$(D\gamma)K^\pm$	$(D\pi^0)\pi^\pm$	$(D\gamma)\pi^\pm$
$K^\pm \pi^\mp$	874 ± 44	536 ± 36	10729 ± 133	7238 ± 119
$\pi\pi$	31 ± 8	15 ± 6	262 ± 20	170 ± 17
KK	101 ± 14	62 ± 12	987 ± 43	709 ± 37
$K_S^0 \pi^0$	86 ± 14	62 ± 11	900 ± 38	583 ± 33
$K_S^0 \omega$	43 ± 11	29 ± 9	419 ± 31	250 ± 24
$K_S^0 \phi$	19 ± 6	21 ± 6	262 ± 22	180 ± 20

expected: $A_{CP^+, \pi}^* = 0.007 \pm 0.029 \pm 0.005$, $A_{CP^-, \pi}^* = 0.032 \pm 0.027 \pm 0.006$ and, for flavor-specific modes, $A_\pi^* = -0.004 \pm 0.010 \pm 0.001$.

We also obtain $R^* = 0.0802 \pm 0.0031 \pm 0.0018$, compatible with the theoretical prediction given in the Introduction, and $(r_B^*)^2 = 0.20 \pm 0.09 \pm 0.03$. We find $\kappa = -0.08 \pm 0.16 \pm 0.02$ [defined in Eq. (12)], consistent with zero as expected. We confirm the large value of $(r_B^*)^2$ that can be inferred from the previous measurements [13] based on the GLW method, with a precision improved by a factor of 2.

Using the value of $\gamma = 67.6 \pm 4.0$ obtained by a SM-based fit of the CKM matrix [33] and the values of r_B^* and δ_B^* from Ref. [18], we predict $A_{CP^+}^* = -0.18 \pm 0.10$, $R_{CP^+}^* = 1.06 \pm 0.06$, $A_{CP^-}^* = 0.20 \pm 0.10$, and $R_{CP^-}^* = 0.98 \pm 0.05$. Our results are compatible with these predictions.

We also compute the Cartesian coordinates with the channel $D \rightarrow K_S^0 \phi$ removed, so as to facilitate the comparison with results obtained with the Dalitz method [18]:

$$\begin{aligned}
 x_+^* &= 0.09 \pm 0.07 \pm 0.02, \\
 x_-^* &= -0.02 \pm 0.06 \pm 0.02, \\
 (r_B^*)^2 &= 0.22 \pm 0.09 \pm 0.03.
 \end{aligned} \tag{18}$$

VIII. SUMMARY

We have performed measurements of the CP eigenmode to flavor-specific mode ratios, and of the CP -violating charge asymmetries of $B^\pm \rightarrow D^* K^\pm$ decays. The ratios R_{CP}^* are found to be compatible with, and more precise

than, previous measurements. Our results for $R_{CP^\pm}^*$ and $A_{CP^\pm}^*$ are at least a factor of 2 more precise than previous measurements [12,13]. The precision of our results for x_\pm^* is comparable to that obtained from Dalitz plot analyses [18,19]. No significant charge asymmetry is observed in the pion modes. These results supersede our previous measurements [12].

ACKNOWLEDGMENTS

We are grateful for the extraordinary contributions of our PEP-II colleagues in achieving the excellent luminosity and machine conditions that have made this work possible. The success of this project also relies critically on the expertise and dedication of the computing organizations that support *BABAR*. The collaborating institutions wish to thank SLAC for its support and the kind hospitality extended to them. This work is supported by the U.S. Department of Energy and National Science Foundation, the Natural Sciences and Engineering Research Council (Canada), the Commissariat à l'Énergie Atomique and Institut National de Physique Nucléaire et de Physique des Particules (France), the Bundesministerium für Bildung und Forschung and Deutsche Forschungsgemeinschaft (Germany), the Istituto Nazionale di Fisica Nucleare (Italy), the Foundation for Fundamental Research on Matter (The Netherlands), the Research Council of Norway, the Ministry of Education and Science of the Russian Federation, Ministerio de Educación y Ciencia (Spain), and the Science and Technology Facilities Council (United Kingdom). Individuals have received support from the Marie-Curie IEF program (European Union) and the A. P. Sloan Foundation.

- [1] N. Cabibbo, Phys. Rev. Lett. **10**, 531 (1963); M. Kobayashi and T. Maskawa, Prog. Theor. Phys. **49**, 652 (1973).
- [2] M. Gronau and D. London, Phys. Lett. B **253**, 483 (1991).
- [3] M. Gronau and D. Wyler, Phys. Lett. B **265**, 172 (1991).
- [4] D. Atwood and A. Soni, Phys. Rev. D **71**, 013007 (2005).
- [5] W.M. Yao *et al.* (Particle Data Group), J. Phys. G **33**, 1 (2006).
- [6] M. Gronau, Phys. Lett. B **557**, 198 (2003).
- [7] B. Aubert *et al.* (BABAR Collaboration), Phys. Rev. Lett. **98**, 211802 (2007).
- [8] M. Staric *et al.* (Belle Collaboration), Phys. Rev. Lett. **98**, 211803 (2007).
- [9] Y. Grossman, A. Soffer, and J. Zupan, Phys. Rev. D **72**, 031501 (2005).
- [10] T.E. Browder, K. Honscheid, and D. Pedrini, Annu. Rev. Nucl. Part. Sci. **46**, 395 (1996).
- [11] C.K. Chua and W.S. Hou, Phys. Rev. D **72**, 036002 (2005).
- [12] B. Aubert *et al.* (BABAR Collaboration), Phys. Rev. D **71**, 031102 (2005).
- [13] K. Abe *et al.* (Belle Collaboration), Phys. Rev. D **73**, 051106 (2006).
- [14] K. Abe *et al.* (Belle Collaboration), Phys. Rev. Lett. **87**, 111801 (2001).
- [15] B. Aubert *et al.* (BABAR Collaboration), Phys. Rev. D **73**, 051105 (2006).
- [16] B. Aubert *et al.* (BABAR Collaboration), Phys. Rev. D **77**, 111102(R) (2008).
- [17] B. Aubert *et al.* (BABAR Collaboration), Phys. Rev. D **72**, 071103 (2005).
- [18] B. Aubert *et al.* (BABAR Collaboration), Phys. Rev. D **78**, 034023 (2008).
- [19] K. Abe *et al.* (Belle Collaboration), arXiv:0803.3375.
- [20] A. Bondar and T. Gershon, Phys. Rev. D **70**, 091503 (2004).
- [21] B. Aubert *et al.* (BABAR Collaboration), Phys. Rev. Lett. **95**, 121802 (2005).
- [22] B. Aubert *et al.* (BABAR Collaboration), Nucl. Instrum. Methods Phys. Res., Sect. A **479**, 1 (2002).
- [23] M. Andreotti (BABAR LST Collaboration), Report No. SLAC-PUB-12205, 2005.
- [24] D.J. Lange, Nucl. Instrum. Methods Phys. Res., Sect. A **462**, 152 (2001).
- [25] S. Agostinelli *et al.* (GEANT4 Collaboration), Nucl. Instrum. Methods Phys. Res., Sect. A **506**, 250 (2003).
- [26] R.A. Fisher, Ann. Eugen. **7**, 179 (1936).
- [27] G.C. Fox and S. Wolfram, Phys. Rev. Lett. **41**, 1581 (1978).
- [28] B. Aubert *et al.* (BABAR Collaboration), Phys. Rev. Lett. **87**, 241801 (2001).
- [29] J. Neyman and E. Pearson, Phil. Trans. R. Soc. A **231**, 289 (1933).
- [30] W. Verkerke and D. Kirkby, arXiv:physics/0306116.
- [31] F. James and M. Roos, Comput. Phys. Commun. **10**, 343 (1975).
- [32] B. Aubert *et al.* (BABAR Collaboration), Phys. Rev. Lett. **99**, 021603 (2007).
- [33] J. Charles *et al.* (CKMfitter Group), Eur. Phys. J. C **41**, 1 (2005), updates at <http://ckmfitter.in2p3.fr>.